Aqueous Foams as Templates for the Synthesis of Calcite Crystal Assemblies of Spherical Morphology

Debabrata Rautaray, Kaustav Sinha, S. Shiv Shankar, Suguna D. Adyanthaya, and Murali Sastry*

Materials Chemistry Division, National Chemical Laboratory, Pune 411 008, India

Received November 18, 2003. Revised Manuscript Received February 2, 2004

The crystallization of calcite in the form of spheroaggregates in aqueous foam stabilized by the surfactant sodium bis-2-ethylhexyl-sulfosuccinate (aerosol OT, AOT) by a method of ion entrapment is described. Reaction of Na_2CO_3 with Ca^{2+} ions electrostatically entrapped in the foam results in the formation of flat, platelike calcite crystals, possibly in the plateau border regions of the foam. Hydrodynamic flow patterns in the foam are believed to transport the calcite platelets from the plateau border regions into the larger plateau junctions where they assemble into spherical structures by hydrophobic association. The large interfacial area of the liquid lamellae in the foam provides an attractive and versatile template for the large-scale synthesis of not only minerals but also other nanoscale materials.

Introduction

Development of experimental strategies for the synthesis of inorganic materials with controllable shape and crystallography is important for application in catalysis, medicine, hybrid materials, ceramics, and cosmetic formulations,[1] and consequently, there is much current interest in the growth of morphologically complex mineral crystals and their morphogenesis. Recognizing that the most complex and exquisite mineral crystallization occurs in biological systems, various biomimetic templates such as Langmuir monolayers,[2−4] self-assembled monolayers (SAMs),[5,6] functionalized polymer surfaces,[7,8] and lipid bilayer stacks[9] have been investigated and show great promise in crystal engineering. Attempts have also been made to control the morphology of crystals nucleated and grown in solution via addition of suitable crystallization inhibitors[10,11] and carrying out of crystal growth in constrained environments such as those afforded by microemulsions[12] and agarose gels.[13]

An exciting and hitherto considerably underexploited dynamic biomimetic template for crystal growth is foam lamellae.[14] Davey and co-workers showed that stabilizing surfactants at the air-bubble/solution interface in foams could be used as nucleation centers for the growth of glycine and $CaCO_3$ crystals.[14] Liquid foams provide an extremely high concentration of gas bubbles dispersed in a liquid and, as a result, yield large interfacial areas populated by the stabilizing surfactant. The bubble-stabilizing surfactants are amphiphiles that assemble at the gas/liquid interface and essentially form extended monolayers akin to Langmuir monolayers that are juxtaposed parallel to each other and separated by a region of water with the polar groups facing inward (Figure 1). These regions occur between two neighboring bubbles and are called the plateau borders while the regions where such plateau borders meet are called the plateau junctions. The close-packed arrangement of polar groups at the gas−liquid interface offers one the possibility of using foams as a template for binding differently charged ions along the plateau borders and junctions and growing a range of inorganic materials by novel chemistry. There is a growing demand for large-scale synthesis of nanoparticles for a variety of large-volume applications (calcite nanoparticles in paper and polymer industries, for example) and we believe the large interfacial area provided by bubbles in a foam could help realize scale-up. As a first step toward using foams for nanoparticle synthesis, Sastry and co-workers have recently shown the synthesis of anisotropic gold nanoparticles in aqueous foams stabilized by the surfactant cetyltrimethylammonium bromide (CTAB).[15] The gold nanoparticles were grown in a two-step process involving the electrostatic binding of $AuCl_4^-$ ions with the cationic CTAB molecules populating the air-bubble/

* To whom correspondence should be addressed. Tel.: +91 20 25893044. Fax: +91 20 25893952/25893044. E-mail: sastry@ems.ncl.res.in.

(1) Matijevic, E. *Curr. Opin. Colloid Interface Sci.* **1996**, *1*, 176.
(2) Heywood, B. R.; Mann, S. *Langmuir* **1992**, *8*, 1492.
(3) Loste, E.; Diaz-Marti, E.; Zarbakhsh, A.; Meldrum, F. C. *Langmuir* **2003**, *19*, 2830.
(4) Rautaray, D.; Sainkar, S. R.; Pavaskar, N. R.; Sastry, M. *CrystEngComm* **2002**, *4*, 626.
(5) Kuther, J.; Nelles, G.; Seshadri, R.; Schaub, M.; Butt, H.-J.; Tremel, W. *Chem. Eur. J.* **1998**, *4*, 1834.
(6) Aizenberg, J.; Black, A. J.; Whitesides, G. M. *J. Am. Chem. Soc.* **1999**, *121*, 4500.
(7) Feng, S.; Bein, T. *Science* **1994**, *265*, 1839.
(8) Park, R. J.; Meldrum, F. C. *Adv. Mater.* **2002**, *14*, 1167.
(9) Damle, C.; Kumar, A.; Bhagwat, S.; Sainkar, S. R.; Sastry, M. *Langmuir* **2002**, *18*, 6075.
(10) Bromley, L. A.; Cottier, D.; Davey, R. J.; Dobbs, B.; Smith, S.; Heywood, B. R. *Langmuir* **1993**, *9*, 3594.
(11) (a) Colfen, H.; Antonietti, M. *Langmuir* **1998**, *14*, 582. (b) Yu, S. H.; Colfen, H.; Hartmann, J.; Antonietti, M. *Adv. Funct. Mater.* **2002**, *12*, 541.
(12) Li, M.; Mann, S. *Langmuir* **2000**, *16*, 7088.
(13) Yang, D.; Qi, L.; Ma, J. *Chem. Commun.* **2003**, 1180.
(14) Dong, B.-D.; Cilliers, J. J.; Davey, R. J.; Garside, J.; Woodburn, E. T. *J. Am. Chem. Soc.* **1998**, *120*, 1625.
(15) Mandal, S.; Arumugam, S. K.; Adyanthaya, S. D.; Pasricha, R.; Sastry, M. *J. Mater. Chem.* **2004**, *14*, 43.

10.1021/cm035182l CCC: $27.50
Published on Web 03/09/2004

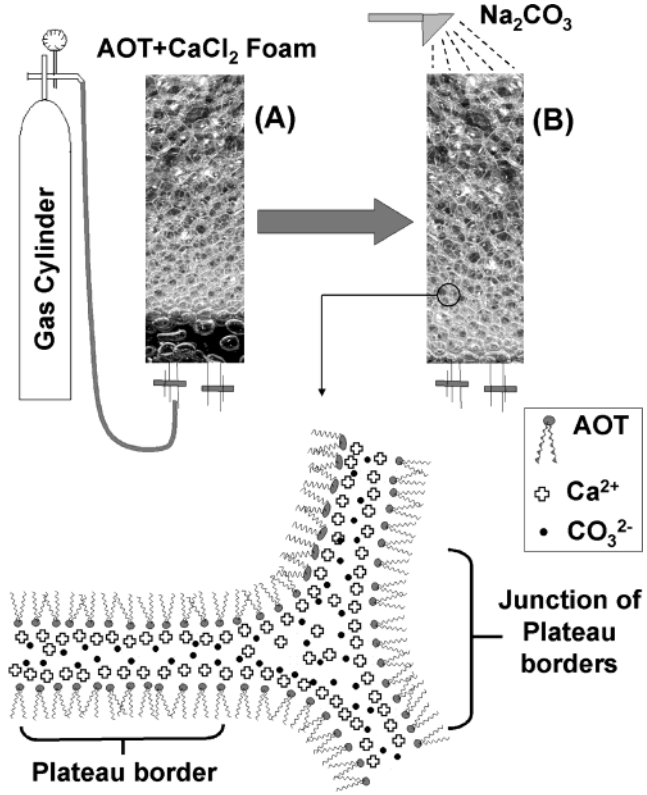

Figure 1. Scheme showing the different steps involved in the synthesis of $CaCO_3$ crystals using aqueous AOT foam and structure of water lamellae in the foam (see text for details).

solution interface followed by the interfacial metal ions by reduction with hydrazine vapors.[15] Gold nanoparticles of variable morphology were formed within different regions of the foam due to reaction cavities of variable thickness present in the foam.

Developing on our first report on foam-based nanoparticle synthesis,[15] we describe herein the formation of spherical assemblies of highly uniform $CaCO_3$ crystals of the calcite polymorph in aqueous foams stabilized by the surfactant aerosol OT (sodium bis-2-ethylhexylsulfosuccinate, AOT). This is accomplished by first electrostatically complexing Ca^{2+} ions with AOT molecules at the air-bubble/solution interface (Figure 1, step A) followed by reaction with Na_2CO_3 solution in the final step (Figure 1, step B). To understand the process of formation of spherical $CaCO_3$ particles better, experiments were performed wherein the structure of the foam was modulated by varying the drainage time of the foam and by creating foams with different bubble sizes. These studies indicate that the calcite crystals of flat, platelike morphology are formed within the plateau borders (Figure 1), following which they assemble into spheroaggregates within the plateau junctions by hydrophobic association. Presented below are details of our study.

Experimental Section

In a typical experiment, a rectangular column of 50-cm height and a square base of 10×10 cm^2 with sintered ceramic disks embedded in it was used for generation of the foam (Figure 1). An aqueous mixture of 50 mL of 5×10^{-2} M calcium chloride and 50 mL of 10^{-2} M AOT was taken in the rectangular column and the foam built up by injecting air at a pressure of 1−5 psig through the ceramic disk (Figure 1, step A). Stable foams of 40-cm height could be routinely

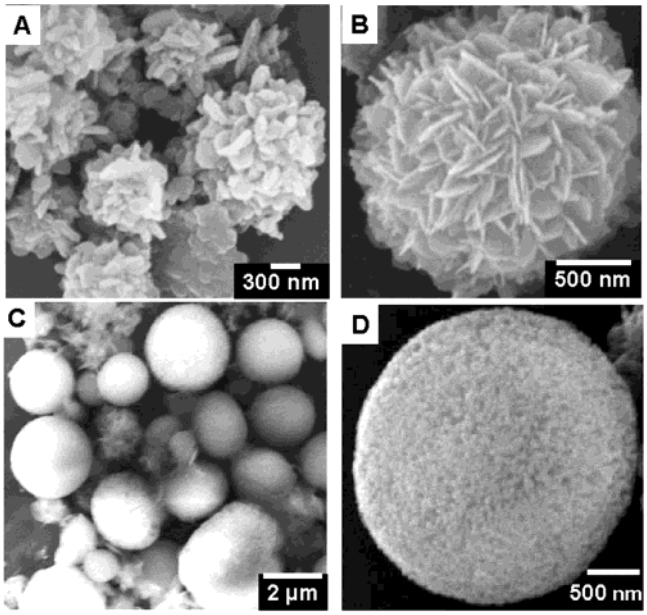

Figure 2. (A−D) SEM images at different magnifications of $CaCO_3$ crystals grown in a foam formed by bubbling air in an aqueous mixture of 5×10^{-2} M $CaCl_2$ and 10^{-2} M AOT and allowing the foam to drain for 10 min. $CaCO_3$ growth was induced by reaction with Na_2CO_3 solution. The bubble size in this experiment was ∼8 mm.

obtained. The liquid lamellae between bubbles in the foam may be considered to consist of two Langmuir monolayers of AOT electrostatically complexed with Ca^{2+} ions (as shown in Figure 1) and therefore amenable to reaction with carbonate anions at the interface. After stabilization of the foam, the aqueous AOT + $CaCl_2$ solution was carefully drained out from below and the foam subjected to a mild and fine spray of aqueous solution of 10^{-3} M sodium carbonate (Figure 1, step B). The foam collapsed gradually (typically 15−20 min after spraying of Na_2CO_3) and the crystals of calcium carbonate were collected through the outlet provided at the bottom of the column.

To understand the process of formation of $CaCO_3$ crystals, their assembly, and relation to the structure of the foam, $CaCO_3$ growth was effected in the foam as described above at different times of drainage of the foam. This was done by carrying out reaction of the $CaCl_2$−AOT foam with Na_2CO_3 solution after allowing 10 min, 30 min, 1 h, 2 h, 4 h, and 5 h of drainage of liquid from the $CaCl_2$−AOT foam. The process of drainage of the water in the foam is expected to lead to variation in the thickness of the water channels in the foam (Figure 1). The structure of the foam may also be modulated by changing the size of the bubbles in the foam. Growth of $CaCO_3$ crystals was also carried out in foams consisting of ∼2- and ∼8-mm bubbles obtained in columns fitted with ceramic disks of different porosity.

Scanning electron microscopy (SEM) and energy-dispersive analysis of X-ray (EDX) measurements of drop-cast films of the $CaCO_3$ crystals grown in the foams deposited on Si(111) substrates were carried out on a Leica Stereoscan-440 SEM equipped with a Phoenix EDX attachment. X-ray diffraction (XRD) analysis of drop-cast films of the $CaCO_3$ crystals grown in the foam deposited on glass substrates was carried out on a Phillips PW 1830 instrument operating at a voltage of 40 kV and a current of 30 mA with Cu Kα radiation. Contact angle measurements of drop-cast films of $CaCO_3$ crystals on glass substrates were carried out by the sessile water-drop method (1-μL water drop) using a Rame-Hart 100 goniometer.

Results and Discussion

Figure 2 shows representative SEM images of $CaCO_3$ crystals synthesized by treating $CaCl_2$−AOT foam of bubble size ∼8 mm with Na_2CO_3 solution after allowing

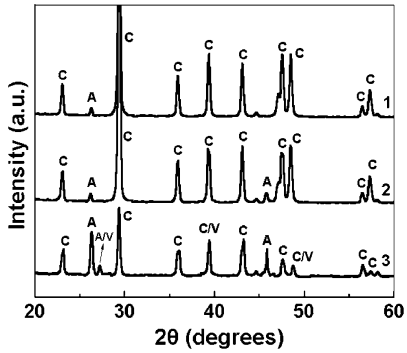

Figure 3. XRD patterns recorded from $CaCO_3$ crystals grown in the aqueous AOT foam after different drainage times. Curve 1, 10 min; curve 2, 1 h; and curve 3, 5 h after drainage (peaks marked with "A" and "V" correspond to aragonite and vaterite Bragg reflections, respectively).

drainage of liquid from the foam for 10 min. A small percentage of the structures were observed to be in the form of fairly open spherical assemblies of flat, platelike crystallites (Figure 2A,B) along with the major percentage of compact spherical calcite particles (Figure 2C). At higher magnification, the surface of the more compact spherical $CaCO_3$ assemblies appears to be made of smaller platelets in a highly close-packed assembly (Figure 2D). An interesting feature of the spherical crystal structures is the uniformity in shape and size (particle diameters in the range 0.6−2 μm). Energy-dispersive analysis of X-rays (EDX) from the crystals shown in Figure 2 yielded strong Ca, C, and O signals together with weaker Na and S signals (data not shown). This indicates the formation of $CaCO_3$ and also the presence of AOT in the spherical structures.

The XRD pattern recorded from the spherical crystal assemblies cast in the form of a film on a glass substrate shows a number of Bragg reflections characteristic of the calcite polymorph along with a small percentage of aragonite (curve 1 in Figure 3).[16] The Bragg reflections marked with "A" correspond to the aragonite polymorph. The peaks are relatively broad, indicating that the observed spherical microparticles of $CaCO_3$ are indeed aggregates/assembly of much smaller crystallites. The XRD results thus conclusively show that both the spherical assembly of flat, plate-shaped $CaCO_3$ crystallites (Figure 2A,B) and the compact, spherical particles (Figure 2C,D) are predominantly of the calcite polymorph.

Figure 4A−C shows high-magnification images of some of the spherical calcite crystals obtained in the foam. All of these spheroaggregates present in different orientations on the Si(111) wafer fortuitously exposed their hollow cores. The $CaCO_3$ crystallites appear to be organized in a radially oriented fashion outward from the hollow center of the spheres. Similar hollow spherical calcite/vaterite crystals have been obtained by Colfen and Antonietti during solution growth of $CaCO_3$ in the presence of suitable double hydrophilic block copolymers (DHBCs).[11] It was speculated that these double-hydrophilic block copolymers, due to their strong interaction with inorganic surfaces, have the potential to control the growth of inorganic crystallites.[11] The formation of hollow cores in the spherical calcite/vaterite crystals were explained as arising due to a recrystallization process during which the core was consumed.[11] We believe a similar process of recrystallization may be operative in this study as well. That this is likely is supported by our observation that the spherical $CaCO_3$ structures in the foam are predominantly of two distinct types—one consisting of spherical assemblies of distinct platelike crystals (Figure 2A,B) while the other set of spherical crystals has a very smooth surface and is made of much more compact crystals (Figure 2C,D). The latter set of compact, smooth spheres (with hollow cores) is possibly the spherical assembly of platelike calcite crystals at an advanced stage of recrystallization. Hollow spheres with prismatic needles along the particle diameter have been observed by Kniep et al. in flourapatite−gelatin composites where growth of fluorapatite starts with the formation of elongated prismatic seeds followed by self-similar branching into anisotropic spherical aggregates, this process being mediated by local electric fields.[17]

The SEM and XRD results indicate that the particles obtained in the foam are composed of smaller calcite crystals self-assembled into spherical superstructures. The flat, platelike calcite crystals are themselves of predominantly two different sizes, leading to open and compact spherical structures. Contact angle measurements of a sessile water drop at different points on the surface of drop-cast films of the calcite particles yielded an average value of 89°. The spherical $CaCO_3$ particles are thus quite hydrophobic, being enveloped by AOT molecules. The presence of AOT on the spheroaggregates suggests that sphere formation occurs through hydrophobic association of AOT-capped calcite platelets during growth of calcite in the aqueous lamellae of the foam. Support for the important role played by the foam is provided by the fact that $CaCO_3$ crystals grown in

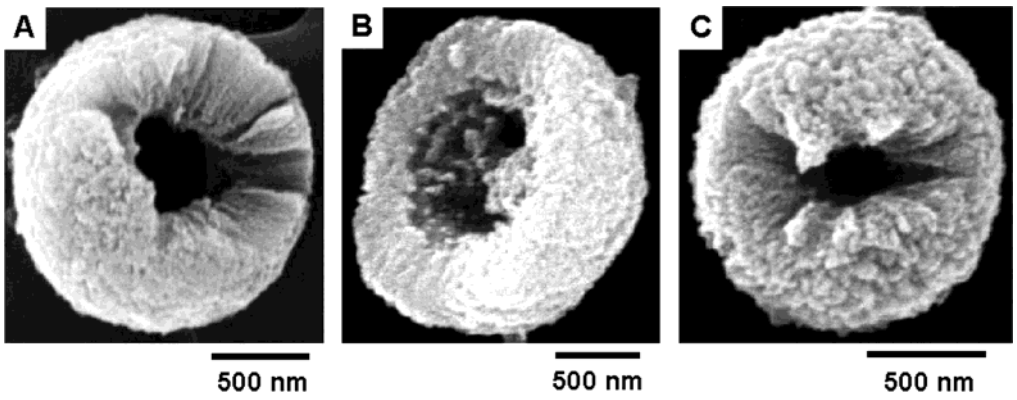

Figure 4. (A−C) SEM images of spherical calcite aggregates grown in the foam, exposing their cores.

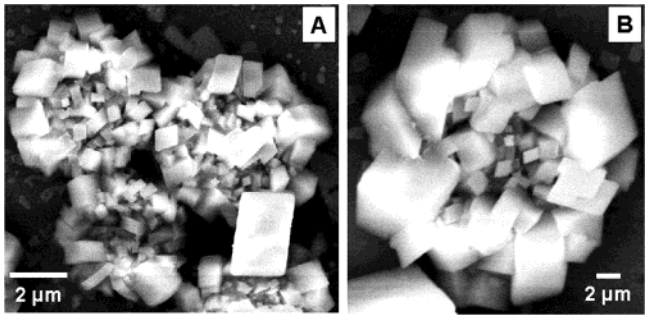

Figure 5. (A and B) SEM images at different magnifications of $CaCO_3$ crystals grown in solution in the presence of 10^{-2} M AOT.

solution by reaction of $CaCl_2$ and Na_2CO_3 in the presence of AOT yielded large, rhombohedral calcite particles assembled into a rudimentary close-packed structure (Figure 5A). The higher magnification SEM image in Figure 5B clearly shows one of the close-packed assemblies of rhombohedral calcite crystals in greater detail with no resemblances to the $CaCO_3$ structures observed in the foam lamellae.

To understand the mechanism leading to $CaCO_3$ assembly into spherical superstructures, the effect of various experimental parameters such as drainage times and bubble sizes on the $CaCO_3$ crystal growth was studied in detail. Figure 6A−F shows SEM images of $CaCO_3$ crystals grown in the foam for 10 min, 30 min, 1 h, 2 h, 4 h, and 5 h after drainage of the foam, respectively. The foam was exceptionally stable even after 5 h of drainage with no evidence for variation in the gross structure (as seen by the naked eye). The $CaCO_3$ crystals grown in the foam after 10 min of drainage (Figure 6A) shows well-defined spherical $CaCO_3$ structures. The inset of Figure 6A shows a relatively solid $CaCO_3$ spheroaggregate with a smooth surface. After 30 min of drainage, $CaCO_3$ spheroids can still be observed along with a number of ill-formed spherical aggregates (Figure 6B). A magnified image of one of the spheroaggregates in this experiment is shown in the inset of Figure 6B, revealing that they are much less compact and more porous than those formed 10 min after drainage (Figure 6A). On progressively increasing the drainage time, we observe that the percentage of spheroaggregates is reduced; they become more coarse and, eventually, yield only flat, platelike $CaCO_3$ crystals with no semblance of hierarchical assembly (Figure 6C−F). Clearly, the drainage time of the foam leads to a dramatic variation in the microscopic structure of the foam and, thereby, the nature of $CaCO_3$ crystals formed in the foam.

The evolution of XRD patterns recorded from the $CaCO_3$ crystals grown in the foam as a function of drainage time is shown in Figure 3 (curve 1, 10 min; curve 2, 1 h; and curve 3, 5 h after drainage), these patterns corresponding to the SEM images shown in parts A, C, and F, respectively, of Figure 6. A number of Bragg reflections are identified and have been indexed with reference to the unit cells of the calcite, aragonite, and vaterite structures.[16] In all the patterns, we observe the presence of calcite and aragonite polymorphs with the presence of a small percentage of vaterite at higher drainage times. The percentage contribution of aragonite appears to increase with increasing foam drainage time. From the SEM images of the $CaCO_3$ crystals grown in these experiments (Figure 6A,C,F), it is difficult to resolve the three phases based purely on crystal morphology considerations. It is thus possible that the $CaCO_3$ platelets observed in Figure 6F are composites of aragonite/vaterite and that the calcite component arises by a process of dissolution and recrystallization of aragonite/vaterite in the foam lamellae/junctions. It is known that vaterite formation in aqueous solution is favored under conditions of high HCO_3^- to Ca^{2+} ratio, whereas calcite is favored at stiochiometric proportions.[18] Under such conditions, positively charged surfaces of $CaCO_3$ are covered with carbonate anions. Thus, a high charge density at the surface could kinetically favor vaterite nuclei through stabilization of disordered clusters of excess charge. It is possible that during spraying of Na_2CO_3 into the Ca^{2+}−AOT foam, an excess of carbonate ions in comparison with calcium ions is temporarily created and thus stabilizes vaterite in the foam lamellae. On this

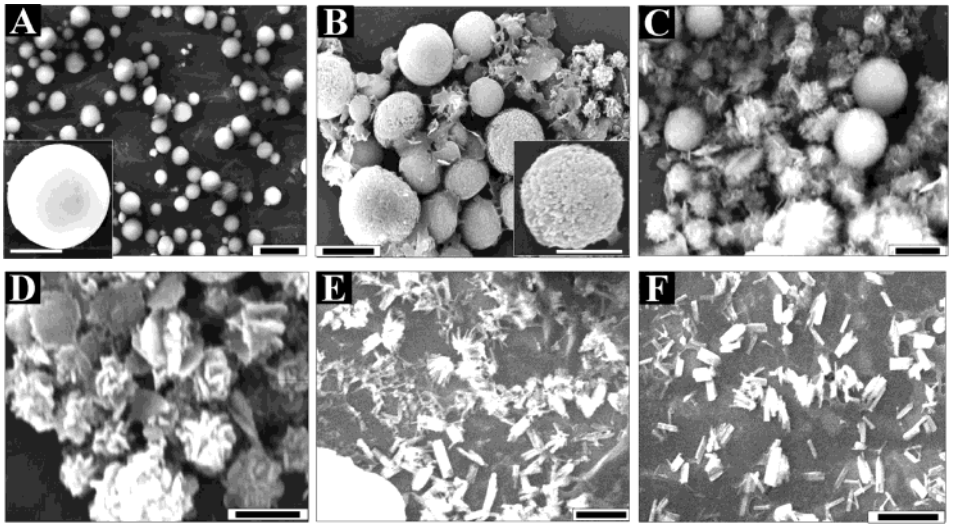

Figure 6. SEM images of $CaCO_3$ crystals grown by reaction of Na_2CO_3 with the Ca^{2+}−AOT foam after different drainage times: (A) 10 min; (B) 30 min; (C) 1 h; (D) 2 h; (E) 3 h; (E) 4 h; and (F) 5 h. The scale bars in all the images correspond to 1 μm while they are 500 nm in the insets.

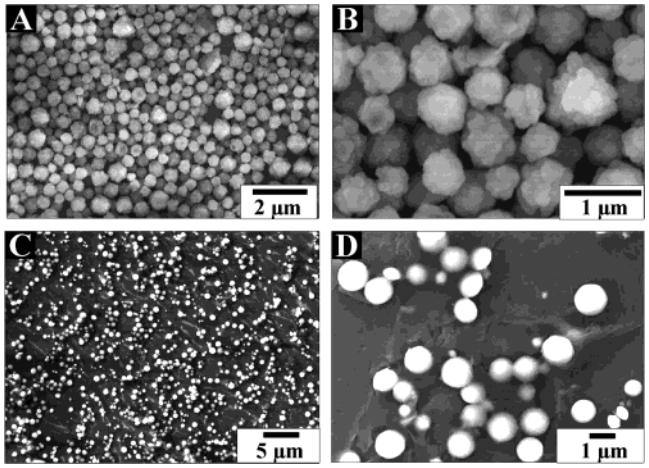

Figure 7. SEM images at different magnification of $CaCO_3$ crystals grown after reaction of Na_2CO_3 with the Ca^{2+}−AOT foam consisting of different size bubbles: (A,B) ∼2 mm and (C, D) ∼8 mm.

basis, the formation of hollow cores in the spherical aggregates may also be explained as arising due to partial dissolution of the vaterite component and recrystallization into calcite.

The effect of bubble size on the morphology of $CaCO_3$ crystals was also studied in foams consisting of ∼2- and ∼8-mm bubbles with a constant drainage period of 10 min in both cases. Figure 7A,B shows SEM images at different magnifications of $CaCO_3$ crystals grown in the foam consisting of 2-mm bubbles while Figure 7C,D corresponds to images obtained from crystals obtained in the 8-mm foam experiment. At low magnification (Figure 7A,C), it is apparent that the density of the $CaCO_3$ spheroaggregates is much higher in the 2-mm bubble experiment. This is understandable given that smaller bubbles in the foam translates into more interfacial bubble area and, consequently, a higher concentration of $CaCO_3$ crystals in the foam. The higher magnification SEM images (Figure 7B,D) show some differences in the $CaCO_3$ spheroaggregates grown in the different foams. While the individual $CaCO_3$ crystals are clearly visible in the spherical aggregates obtained in the 2-mm foam (Figure 7B), the surface of the spheroaggregates in the 8-mm foam is much smoother (Figure 7D). It may be noted that, with change in bubble size, even though the interfacial bubble area changes, there is no significant change in the thickness of the plateau borders and the cross-sectional area of the plateau junctions. The thickness of the plateau borders and the dimensions of the plateau junctions is observed to change only as a function of time of drainage of the foam and not so critically on the bubble size. At this stage, it is not clear what the difference in surface texture of the spheroaggregates is due to and how it correlates with the bubble size in the foam.

Experiments were also carried out by changing the concentration of Ca^{2+} ions and keeping the concentration of AOT (10^{-2} M) constant. At higher concentration of Ca^{2+} ions (10^{-1} M) in the foaming solution, the foam was observed to be very unstable with collapse of foam taking place within 5 min of its formation. At lower concentration of Ca^{2+} ions (10^{-2} M), although the stability of the foam was better, good spherical $CaCO_3$ spheroaggregates were not observed to form (Supporting Information, S1). On the basis of these observations, a concentration of 5×10^{-2} M Ca^{2+} ions and 10^{-2} M AOT was established as optimum for the formation of $CaCO_3$ spheroaggregates.

On the basis of the above studies, we believe formation of $CaCO_3$ spheroids consisting of flat, platelike calcite subunits arises from a mesoscale self-assembly process[19] as described below. The collapse of the foam consequent to Na_2CO_3 treatment and $CaCO_3$ formation is quite slow (ca. 15−20-min collapse time) and hence it may be reasonably assumed that the assembly of spheroaggregates of flat calcite platelets does not occur during collapse of the foam. The formation of the calcite platelets and assembly into spherical superstructures therefore takes place in the intact foam lamellae. The presence of AOT on the surface of the calcite spheroaggregates inferred from the contact angle measurements indicates that hydrophobic interactions between the AOT-capped calcite platelets is responsible for the assembly, possibly in the following manner. The plateau borders shown in Figure 1 provide an anisotropic confinement to the solution trapped between them and also act as planar charged templates for immobilizing oppositely charged species. Comparatively, the plateau junctions encompass a greater volume of solution and are more isotropic in spatial extent. The thickness of both the plateau borders and the plateau junctions decreases with increasing time of drainage as the foam dries. As mirrored by the SEM images (Figure 2A,B), the $CaCO_3$ platelets constituting the spherical aggregates are most likely synthesized in the plateau border regions. During treatment of the foam with Na_2CO_3 solution, we believe that hydrodynamic flow of the liquid through the foam by capillary action drives the calcite platelets synthesized in the plateau regions to the more capacious plateau junctions where they aggregate via hydrophobic association. Hydrophobic forces being nondirectional, the aggregates tend to attain a spherical morphology, this structure being the most energy-conserving. This is also evidenced from the morphology of the $CaCO_3$ particles synthesized in AOT foam after different times of drainage. At lower times of drainage (10 and 30 min) when the plateau border regions contain a greater amount of entrapped water, hydrodynamic flow during treatment with Na_2CO_3 drives the platelets formed in these regions to the plateau junctions where they become aggregated, whereas at higher drainage times, the plateau borders are thin and consequently hydrodynamic flow is minimized in the plateau border regions. Formation of the smooth surfaced compact spherical particles could be a result of further growth of calcite on the aggregated $CaCO_3$ spherical particles. It is expected that, at lower drainage times, more Ca^{2+} ions are present in the foam lamellae along with water that would be available for secondary growth on the spheroaggregates. This pos-

(16) The XRD patterns were indexed with reference to the unit cell of the calcite and aragonite structure from *ASTM* chart card nos. 5-0586 and 5-0453, respectively.

(17) Busch, S.; Dolhaine, H.; Duchesne, A.; Heinz, S.; Hochrein, O.; Laeri, F.; Podebrad, O.; Vietze, U.; Weiland, T.; Kniep, R. *Eur. J. Inorg. Chem.* **1999**, 1643.

(18) Naka, K.; Chujo, Y. *Chem. Mater.* **2001**, *13*, 3245.

(19) Yu, S. H.; Colfen, H.; Xu, A. W.; Dong, W. *Cryst. Growth Des.* **2004**, *4*, 33.

sibly leads to the observed increase in porosity with increasing drainage time scales in the $CaCl_2$−AOT foam and is supported by the fact that the size of most of the spherical aggregates that are clearly visible as aggregates of platelets is less than the size of the smooth surfaced spherical particles. Thus, the dynamic nature of the foam lamellae does play a crucial role in yielding spherical calcite particles since such structures have not been observed in $CaCO_3$ crystallization at static interfaces such as Langmuir monolayers.[3] Though we believe this to be the mechanism and is thus at this time-speculative, studies are under progress to establish and understand in detail the microstructure of the foam lamellae and the dynamics involved in it. As mentioned briefly earlier, the formation of vaterite crystals (with spherical morphology) and aragonite crystals followed by their recrytallization into calcite could provide an alternative mechanism for the formation of spheroaggregates of calcite and would need to be discounted.

To summarize, formation of flat, platelike calcite crystals and their hierarchical assembly into uniform spherical aggregates in an aqueous foam stabilized by the surfactant aerosol OT has been described. A combination of extremely large interfacial templating area provided by the liquid lamellae in foams stabilized by ionizable surfactants and the dynamic nature of the foam bubbles makes this method potentially exciting for the large-scale synthesis of other inorganic materials (nanomaterials) and minerals.

Acknowledgment. D.R. and S.S.S. thank the Department of Science and Technology (DST) and Council of Scientific and Industrial Research (CSIR), Govt. of India, for research fellowships. We are grateful to Dr. Sudhakar Sainkar for providing SEM facilities.

Supporting Information Available: SEM image of $CaCO_3$ crystals grown in a foam formed by bubbling air in an aqueous mixture of 10^{-2} M $CaCl_2$ and 10^{-2} M AOT and allowing the foam to drain for 10 min; $CaCO_3$ growth was induced by reaction with Na_2CO_3 solution and the bubble size in this experiment was ∼8 mm (PDF). This material is available free of charge via the Internet at http://pubs.acs.org.

CM035182L